

# Newsletter

## Issue 20, June 2019 Contents

President Report .....1  
 Nonlinear Model Updating based on Dynamic Response Decomposition .....7  
 A Technical Note on Remote Sensing for Bridge Monitoring .....19  
 Conference News .....28

President Message  
*Tommy Chan*

*Professor in Civil Engineering, Queensland University of Technology*

Dear All,

Last year, when I was preparing the President Message for the June Issue of our Newsletter (Issue 16, 2018), I was also preparing the flyer for our proposed ARC Industrial Transformation Training Centre for SHM (ATCSHM). At that time, I collected a lot of information about the bridge collapses all over the world, when the latest collapse was the collapse of the Florida International University (FIU) Bridge on 15 March 2018 killing 6 people. Then on 14 August, another bridge collapse tragedy (Collapse of the Morandi Bridge, Italy) happened in Italy killing more people. I commented previously that the FIU Bridge used a new material, self-cleaning concrete and a new construction method, adopting the so-called ABC (Accelerated Bridge Construction) technology. The Morandi Bridge was also a new design at its time. These collapses alert us that we need to know more about the actual behaviour and performance of new materials, new designs of structural systems and new construction methods, in both the short and long terms with SHM systems installed in new types of infrastructure, we are better able to gather performance information and gain a better understanding of their behaviour. This will not only enhance infrastructure safety during the early stages of construction but will also provide new information to validate the design assumptions as well as to improve future designs.



# Newsletter

Civil infrastructure, such as buildings, bridges, roads, dams and tunnels; and energy infrastructure, such as gas pipelines, oil platforms and wind turbines are built to last several decades. However, we are well aware that during their service lives, progressive deterioration and sudden damage can occur due to changes in vehicle loads, environmental effects and random events such as impacts and earthquakes. For example, increases in traffic speed and loads can accelerate the deterioration of ageing bridges leading to structural failure which causes disruption in the transport system and economic losses. Retrofitting and/or reconstruction of failed infrastructure involve large costs for infrastructure owners. The majority of infrastructure that Australians will use in the next 15 years (and indeed the next 50 years) has already been built. However, this infrastructure will require substantial additional funding for maintenance, renewal and upgrade as population and usage grows. Moreover, it has been observed that sections of Australia’s infrastructure asset are already in poor or declining condition. These significant engineering challenges can be addressed through health monitoring which can track infrastructure safety and detect the onset of damage in a timely manner to enable appropriate retrofitting to be carried out, thereby protecting our national infrastructure systems. Furthermore, to achieve cost-effective, durable and efficient infrastructure for the future, it is critical to test, adjust and select the best material science solutions, to inform the efficient design and manufacture of new advanced construction materials and components. Therefore, to achieve all these benefits, the establishment of the proposed Training Centre (ATCSHM) is necessary and timely. Actually, the year 2018 is one of the years with high number of bridge collapses with at least 10 bridge collapses in the year. These 10 bridge collapses happened all over the world, with 3 in America (1 in Central America, 1 in North America, 1 in South America), 5 in Asia, 2 in Europe, killing more than 73 people. Two of them were collapsed during construction, and some were caused by design flaw and some were caused by ageing bridges with too heavy vehicle.

Australia also has a number of bridge collapses in its history. Below is a table showing at least 6 bridge collapses, partial or fully, happened previously.

Year	Location/Bridge	State	No. Killed	Possible Cause	Reference
1926	Fremantle Railroad Bridge	WA	Nil	Flood	<a href="https://trove.nla.gov.au/newspaper/article/51361959">https://trove.nla.gov.au/newspaper/article/51361959</a>
1962	King Street Bridge	VIC	Nil	Toe Cracks developed after welding without being discovered during construction	<a href="https://web.archive.org/web/20130516080709/http://prov.vic.gov.au/wp-content/uploads/2012/02/VPARL1963-64No11.pdf">https://web.archive.org/web/20130516080709/http://prov.vic.gov.au/wp-content/uploads/2012/02/VPARL1963-64No11.pdf</a>



# Newsletter

1970	West Gate Bridge	VIC	35	Collapse during construction	<a href="https://www.theage.com.au/national/victoria/forty-years-on-the-west-gate-bridge-collapse-still-looms-large-20101015-16nlo.html">https://www.theage.com.au/national/victoria/forty-years-on-the-west-gate-bridge-collapse-still-looms-large-20101015-16nlo.html</a>
1975	Tasman Bridge	TAS	12	Ore freighter collided with pylons	<a href="https://web.archive.org/web/20120317061918/http://www.em.gov.au/Documents/Tasman_Bridge_disaster_25th_anniversary_memorial_service.pdf">https://web.archive.org/web/20120317061918/http://www.em.gov.au/Documents/Tasman_Bridge_disaster_25th_anniversary_memorial_service.pdf</a>
1977	Granville Railway Bridge	NSW	84	Derailed train collided with a pier	<a href="http://www.granvillehistorical.org.au/granville-history.php">http://www.granvillehistorical.org.au/granville-history.php</a>
2007	Gosford Culvert	NSW	5	A culvert collapsed	<a href="https://www.smh.com.au/national/culvert-tragedy-coroner-blames-council-20080919-gdsvgs.html">https://www.smh.com.au/national/culvert-tragedy-coroner-blames-council-20080919-gdsvgs.html</a>

It can be seen that similar to other countries, the collapses could be caused by inappropriate inspection, design or protection. It could be seen that SHM could be very helpful to improve that.

Every time after this kind of accidents, we have some lessons learnt. However, can we do better to avoid the followings?

- Families lost their beloved ones
- Engineers lost their image
- Public lost their trust in using infrastructures
- Connection lost
- Productivity lost
- ...

For that reason, in the past 10 years, ANSHM has been working hard to promote the SHM technologies, especially its implementation within the country.

One of the great achievements that ANSHM produced is having the latest Australian Bridge Design Standards (AS5100), released in March 2017, include a section on Structural Health Monitoring (SHM). However, it is just the first step. SHM can help improve the safety and operation of infrastructure systems economically, efficiently and intelligently. In turn, the monitored data can be used to improve the design of advanced construction materials and structural components from the analysis of quantitative data and the developed physics-based models or data-driven models. The ATCSHM will help more effective SHM systems implemented in Australia to help reduce the



# Newsletter

monitoring and maintenance costs of infrastructures, and at the same time providing greater service life of infrastructure, greater public safety, greater production efficiency, and better design.

Below are the updates of the month.

## **ATCSHM Proposal**

According to the Key dates for Industrial Transformation Training Centres 2019 shown on the ARC Official Webpage, the anticipated announcement of the outcomes of the ITTC proposals in the latest round is scheduled in the Third Quarter 2019. Last year, it was announced in August 2018. In the past, it could be announced earlier. Anyway, as mentioned earlier, please keep lobbying the ATCSHM of ANSHM to anyone you think who may be a panel member. Please try your best to help promote the establishment of the ATCSHM, not only for the benefits of ANSHM, but also for the benefits and safety of the country. It could be seen from what I wrote above, establishing such a training Centre is timely and crucial for the practical implementation of this technology for reduced frequency of operational disruption, maintenance and rehabilitation costs; improved design and construction efficiency; and enhanced safety and performance of infrastructure.

Actually, the needs of SHM have been realised by more and more asset owners and maintenance teams of various infrastructures. Just for this month (May), I have received at least three inquiries from the industry about how ANSHM could help them implement SHM systems for their assets or their clients. I also noticed two of the recent CRC proposals both include a component on SHM. I am so pleased to know that more and more from the Industry consider the importance of SHM and include it as a component to monitor their assets and operations, agreeing that SHM will be a solution to many of their problems. This will make their proposals to be more complete. It also confirms the significance of the establishment of our ATCSHM as it is more comprehensive and directly focus at how SHM could be useful in different aspects as well as enhancing academic and industry collaboration and industry training.

## **ANSHM 11<sup>th</sup> Annual Workshop**

I am pleased to inform you that we have confirmed the date for the ANSHM 11<sup>th</sup> Annual Workshop. It will be hosted by Griffith University, held at their Gold Coast Campus from 2 – 3 December 2019. Please pencil it down in your calendar so that you will not miss this ANSHM important annual event. You should have received the First Announcement sent by Prof Hong Guan and Dr. Domic Ong. They have also created a very informative Website for the workshop (<https://www.griffith.edu.au/cities-research-institute/news-and-events/seminars-and-events/11th-anshm-annual-workshop>). You can find all the details including the venue, key dates, Call for Abstracts,

# Newsletter

tentative program, travel and accommodation options, and contact details from the website. Many thanks to Hong and her team for working so hard to this ANSHM important annual event.

We received a few inquiries about how many presentations that one university could have. In the past ANSHM workshops, it is our tradition that each university could have only one presentation. Actually, it also depends on how many presentations that we could accommodate. We will discuss that in our next EC meeting.

## **ANSHM Technical Workshop**

Earlier the year, we were approached by a company asking us to provide training to their engineers on SHM. We consider that as a great opportunity as it aligns well with our objectives to *raise general community awareness on the need for and value of SHM research and application*. Therefore, in the last Executive Committee meeting, we appointed A/Prof Xinqun Zhu to co-organise it with the company as the technical workshop we co-organised with VicRoads last year. Similar to the VicRoads/ANSHM Technical Workshop, it will be on the basic technical aspects of SHM about its values, its background and how to practically apply the technologies related to SHM for monitoring the structural health, rather than the latest research and development as we normally do in our annual workshop. We are working on the venue, the date of the workshop and other details. We will keep you informed about this technical workshop in due course.

## **Special Sessions/Mini Symposia**

### *EASEC-16*

We have received five abstracts so far for the ANSHM special session “Recent Research Advances on Innovative Techniques for Structural Health Monitoring” in the *16th East Asia-Pacific Conference on Structural Engineering & Construction (EASEC-16)*, which will be held in Brisbane, Australia on 3rd-6th Dec 2019 (<https://easec16.com.au/>). So far 5 abstracts have been accepted. The deadline to submit full papers is due 1 July 2019. If you are still interested in attending this session, you are most welcome to submit the full paper to [Junli@curtin.edu.au](mailto:Junli@curtin.edu.au) or [qzkong123@gmail.com](mailto:qzkong123@gmail.com) by 1 July 2019.

### *IPDO2019*

Another ANSHM Mini Symposium is “Recent regularization methods for dynamic load identification” (<http://ipdo2019.ipdos.org/Minisymposiums.html>) in the Fifth International Symposium on Inverse Problems, Design and Optimization (IPDO2019) which will be held in Holiday Inn Riverside, Tianjin, China, during September 24-26, 2019. Anyone who is interested to present at this MS, please send me a message.

# Newsletter

## **ANSHM Special Issue**

As mentioned in the last update that we are preparing to have a special issue for the presentations at the 10<sup>th</sup> ANSHM Workshop as well as the ANSHM Special Session in ACMSM25. We also plan to have this special issue to celebrate our 10<sup>th</sup> Anniversary. Its editors will be Yu Tao, Jun Li, Andy Nguyen and myself. Jun and Andy are preparing proposals to be submitted to two international journals for their consideration. More details and call for abstracts will be forwarded in due course.

## **Executive Committee Meeting**

We will have our next Executive Committee Meeting to be held around mid-June. There will be a lot to be discussed, including Web forum, 11<sup>th</sup> ANSHM, the technical workshop, research collaboration, collection of articles for the Newsletter, preparation of technical notes as requested in the last two industry forums, external affairs, how we celebrate the 10<sup>th</sup> Anniversary, the achievements we made in the past 10 years, etc. You are also welcome to suggest some issues to be discussed. If so, please send me a message for an item to be included in the next EC meeting by 5 June 2019.

## **Highlight of this Issue**

This issue is edited by Mehrisadat Makki Alamdari. As mentioned earlier, we will try to include more technical notes in our Newsletter for the industry to better understand SHM in a 'down to earth' manner. Mehrisadat has tried her best to include another technical note in this issue, *Remote Sensing for Bridge Monitoring*. Many thanks to Mehri for her effort. Besides, there is also an interesting research article by Yu Xin, Jun Li and Hong Hao of Curtin University, reporting their research on nonlinear model updating using the instantaneous amplitudes of the decomposed dynamic responses.

With kind regards,

Tommy Chan

President, ANSHM

[www.ANSHM.org.au](http://www.ANSHM.org.au)

# Newsletter

## Nonlinear Model Updating based on Dynamic Response Decomposition

Yu Xin, Jun Li and Hong Hao

Center for Infrastructural Monitoring and Protection, School of Civil and Mechanical Engineering, Curtin University, Australia

**Abstract:** This paper proposes a nonlinear model updating approach using the instantaneous amplitudes of the decomposed dynamic responses. Uncertainty quantification of the model updating results considering the effect of the measurement noise is conducted. The residual of the instantaneous amplitudes of the decomposed structural dynamic responses between the test structure and the analytical nonlinear model is used to construct the maximum likelihood function. Numerical studies on a three-story nonlinear shear type building under earthquake excitations are performed to verify the accuracy and performance of the proposed approach. Numerical results demonstrate that the proposed approach is reliable and accurate for nonlinear model updating.

**Keywords:** Nonlinear model, Instantaneous amplitudes, updating.

### Introduction

Studies on developing reliable finite element model updating methods have been gained increasing attentions from engineers and researchers, and various techniques have been developed (Friswell et al. 1995) and successfully applied for linear and nonlinear model updating (Hemez et al. 2014). This process is mainly based on minimizing the difference between the quantitative structural characteristics obtained from the measured data and the analytical structural model by adjusting the structural model parameters. Since the number of measured structural response parameters is always less than the actual structural parameters in a finite element model, optimization analysis is needed in performing model updating. The accuracy of deterministic model updating results depends on the accuracy of the initial structural model and the accuracy of the structural response characteristics extracted from the measured data (Noel et al. 2017). However, for deterministic model updating methods, the effect of uncertainties on the model updating results needs to be carefully considered. The uncertainties in the model updating usually arise from the measurement noise in the response data and the modeling errors in the structure. Accounting for the propagation effect of these uncertainties on the model updating process and results have attracted significant attention in recent years (Xia et al. 2002).

One possible approach to deal with these uncertainties in model updating is using a probabilistic framework based on the well-known Bayesian theorem (Simoen et al. 2013 & Yuen et al. 2011). The

# Newsletter

initial Bayesian approach for parameter estimation in model updating considering uncertainty was developed (Beck et al. 1998 & Katafygiotis et al. 1998). Behmanesh et al. (2015) proposed a hierarchical Bayesian FEMU method for uncertainty quantification and damage identification of structural systems. Wan et al. (2015) proposed using an efficient Bayesian inference method with delayed rejection adaptive Metropolis (DRAM) algorithm to refine the FEM of a four-span pedestrian bridge considering the uncertainty in identified modal properties.

This paper proposes using a nonlinear model updating approach based on the instantaneous amplitudes of the decomposed dynamic responses. The uncertainty effect from the measurement noise in response data is considered. The instantaneous parameters of mono-components are firstly extracted from the response signal by using analytical mode decomposed (AMD) method (Wang et al. 2013) and Hilbert Transform. The nonlinear model parameter updating problem is formulated as the Maximum Likelihood Estimation (MLE). The optimization problem of MLE is solved with a gradient-based interior point algorithm (Byrd et al. 2004), and the uncertainty quantification of the identified nonlinear model parameters is conducted by using the Cram-Rao lower bound (CRLB) theorem (Kay et al. 1993). To validate the accuracy and effectiveness of the proposed nonlinear model updating approach, numerical studies on a three-story nonlinear shear type structure under the earthquake excitation are conducted.

## Theory

### Time frequency analysis

For an  $n$  DOF nonlinear system, the equation of motion can be written as

$$\mathbf{M}(t)\ddot{\mathbf{x}}(t) + \mathbf{C}(t)\dot{\mathbf{x}}(t) + \mathbf{K}(t)\mathbf{x}(t) = \mathbf{f}(t) \quad (1)$$

in which  $\mathbf{M}(t)$ ,  $\mathbf{C}(t)$  and  $\mathbf{K}(t)$  are time-varying mass, damping, and stiffness matrices, respectively.  $\mathbf{f}(t)$  is the excitation force vector. For a nonlinear structure, the nonlinear restoring force as function of time can be transformed into a multiplication form  $\mathbf{K}(t)\mathbf{x}(t)$  with a new time-varying stiffness matrix  $\mathbf{K}(t)$  and a system solution  $\mathbf{x}(t)$  with an overlapping spectrum (Feldman, 1994). Similarly, the nonlinear damping force can also be transformed into a function of time as a multiplication  $\mathbf{C}(t)\dot{\mathbf{x}}(t)$  between the time-varying damping coefficient matrix  $\mathbf{C}(t)$  and the velocity  $\dot{\mathbf{x}}(t)$ .

# Newsletter

Dynamic responses of Eq. (1) can be taken as a combination of several mono-components with time-varying frequency and amplitude. The measured response of the  $l$ th degree  $x_l(t)$  can be expressed as the function of mono-component  $x_l^{(i)}(t)$

$$x_l(t) = \sum_{i=1}^n x_l^{(i)}(t) \quad (2)$$

Since the frequencies of the responses of a nonlinear structure often change with time, the extended AMD (Wang et al. 2013) is used to decompose the time-varying vibration signal.

The analytical signal  $z_l^{(i)}$  of the  $i$ th decomposed response  $x_l^{(i)}(t)$  can be expressed as

$$z_l^{(i)} = x_l^{(i)}(t) + H[x_l^{(i)}(t)]A_i(t)e^{j\int \omega_i(t)dt} \quad (3)$$

in which  $A_i(t)$  and  $\omega_i(t)$  are the instantaneous amplitude and frequency of a decomposed non-stationary signal  $z_l^{(i)}$ , respectively. In Eq. (3),  $A_i(t)$  represents the amplitude information of  $z_l^{(i)}$ , and  $\omega_i(t)$  reflects the instantaneous phase information of the decomposed signal. The instantaneous frequency and amplitude can be used to describe the characteristics of a non-stationary signal.

## Nonlinear model updating and uncertainty quantification

In this section, instantaneous amplitudes extracted from measured acceleration responses are used for nonlinear model updating. The identified instantaneous parameters of acceleration responses can be expressed as

$$A_{acc}(t) = [A_1(t), A_2(t), \dots, A_m(t)]_{t \times m}^T \quad (4)$$

where  $A_m(t)$  is the instantaneous acceleration amplitude of the  $m$ th mono-component at the time instant  $t$ .

# Newsletter

The instantaneous amplitudes  $A_{acc}(t)$  extracted from the measured acceleration responses may be different from those calculated from the analytical responses with the structural finite element model. The difference can be defined as

$$\boldsymbol{\varepsilon}^m(\boldsymbol{\theta}, t) = A_{acc}(t) - A_{acc}(\boldsymbol{\theta}, t) \quad (5)$$

$$A_{acc}(\boldsymbol{\theta}, t) = [A_1(\boldsymbol{\theta}, t), A_2(\boldsymbol{\theta}, t), \dots, A_m(\boldsymbol{\theta}, t)]_{t \times m}^T \quad (6)$$

in which  $\boldsymbol{\theta}$  is the vector of nonlinear model parameters,  $A_{acc}(\boldsymbol{\theta}, t)$  is the instantaneous amplitude vector identified from measured acceleration response, and  $\boldsymbol{\varepsilon}^m(\boldsymbol{\theta}, t)$  represents the difference in the instantaneous amplitudes between the test and analytical results. Generally, the residual  $\boldsymbol{\varepsilon}^m(\boldsymbol{\theta}, t)$  mainly stems from measurement noise and modeling error (Simoen et al. 2013 & Yuen et al. 2011). The measurement noises in the recorded acceleration responses are assumed as stationary and independent Gaussian white noises with zero means. Therefore, the difference vector  $\boldsymbol{\varepsilon}^m(\boldsymbol{\theta}, t)$  could also be considered as a Gaussian white noise process. Based on this assumption, the nonlinear model updating can be formulated as the following optimization problem

$$\begin{aligned} \hat{\boldsymbol{\theta}} &= \arg \min \left\{ \sum_{m=1}^{N_m} \sum_{t=1}^{N_t} \text{trace}(\boldsymbol{\varepsilon}^m(t) \boldsymbol{\varepsilon}^m(\boldsymbol{\theta}, t)^T) \right\} \\ &= \arg \min \left\{ \sum_{m=1}^{N_m} \sum_{t=1}^{N_t} \|A_m(t) - A_m(\boldsymbol{\theta}, t)\| \right\} \end{aligned} \quad (7)$$

Solving the optimization problem as shown in Eq. (7) can be derived based on Bayesian framework and the MLE methods when a Gaussian white noise simulation error is assumed (Yuen et al. 2011). Therefore, the unknown model parameters  $\boldsymbol{\theta}$  in Eq. (7) can be considered as stochastic variables based on Bayesian strategy for parameter estimation. External excitation information on the structures is assumed available for the nonlinear model updating in this study.

The residuals in the instantaneous amplitudes extracted from acceleration responses between measured data and the analytical nonlinear model can be considered as a Gaussian white noise process with  $\boldsymbol{\varepsilon} \sim N(0, \boldsymbol{\Sigma}_\varepsilon)$ . MLE of  $\boldsymbol{\theta}$  can be expressed as

$$\hat{\boldsymbol{\theta}} = \arg \min \left\{ \frac{N_m N_t}{2} \ln(|\boldsymbol{\Sigma}_\varepsilon|) + \frac{1}{2} \sum_{m=1}^{N_m} \sum_{t=1}^{N_t} (A_m(t) - A_m(\boldsymbol{\theta}, t))^T \boldsymbol{\Sigma}_\varepsilon^{-1} (A_m(t) - A_m(\boldsymbol{\theta}, t)) \right\} \quad (8)$$

# Newsletter

The parameter estimation problem in Eq. (8) can be transformed as a constrained nonlinear optimization problem by setting a feasibility range for the nonlinear model parameters and the initial error variances (i.e.,  $\theta_{min} \leq \theta \leq \theta_{max}$  and  $\sigma_{min}^2 \leq \sigma^2 \leq \sigma_{max}^2$ ). This optimization problem is solved by using a gradient-based interior point method (Byrd et al. 2004), and the optimization algorithm is available in the MATLAB optimization toolbox (MATLAB, 2017a).

After the nonlinear modal parameters  $\theta$  and error variances of the instantaneous acceleration amplitudes  $\sigma_{N_m}^2$ , CRLB method is used to quantify the uncertainty effect based on the obtained  $\hat{\theta}$  and

$\hat{\sigma}_{N_m}^2$  from the Bayesian nonlinear model updating approach.

## Numerical Verification

### Instantaneous parameters identification

The finite element model of a two-dimensional three-story nonlinear shear frame, as shown in Fig. 1, is built by using finite element analysis software Opensees. The height of the frame column in each story is 3m, with a total length of 9m, and the length of all beams are set as 6m. The fiber section is selected to define all column and beam elements, and the detailed size of cross-sections are shown in Fig. 1. In this simulation, the columns of the first-story are defined as Bouc-wen hysteretic material model (Wang et al. 2015 & Ikhoulane et al. 2007), and others columns and beams are defined as linear-elastic components. The Bouc-Wen model parameters are defined as  $\alpha = 0.3, \beta = 180, \gamma = 180, \delta_\eta = 1.2, \delta_\nu = 0.15, n=1$  and  $A=1$ . In the Bouc-Wen model,  $\alpha$  represents the ratio of the post-yield stiffness to the initial elastic stiffness;  $A, \beta$  and  $\gamma$  control the shape of hysteresis loop;  $\delta_\eta$  and  $\delta_\nu$  affect the degradation of material;  $n$  is a parameter that controls the transition from linear to nonlinear range. The WHOX longitudinal component from the Northridge 1994 ground motion record, as presented in Fig. 2, is selected as the applied external excitation on the model. The obtained acceleration response on the top floor is assumed as the measured dynamic response with a sampling rate of 240Hz, as shown in Fig. 3, and will be used for the signal decomposition. By using the procedure described in Section 2.1, the identified instantaneous amplitudes of the first and second mono-components from the acceleration response on the top floor are shown in Figs. 4(a) and Fig.

# Newsletter

4(b), respectively. The identified instantaneous frequencies of the first two mono-components are shown in Fig. 5 with the slowly-varying components of the identified instantaneous frequencies denoted with solid lines, which represent the nonlinear structural behavior and can be obtained by filtering out the fast-varying part with AMD method.

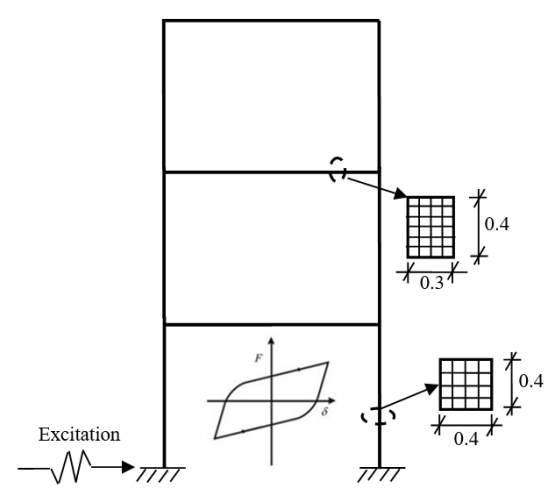


**Fig. 1.** A three-story nonlinear model simulated in Opensees.

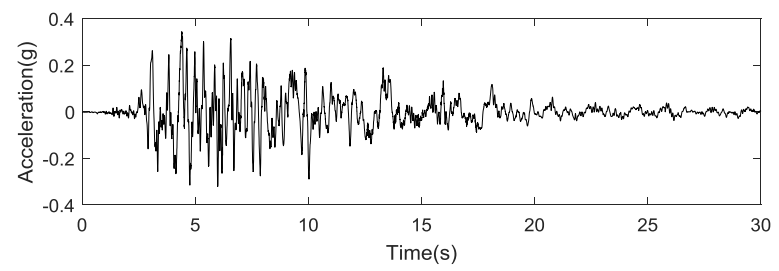


**Fig. 2.** Acceleration record of Northridge earthquake.

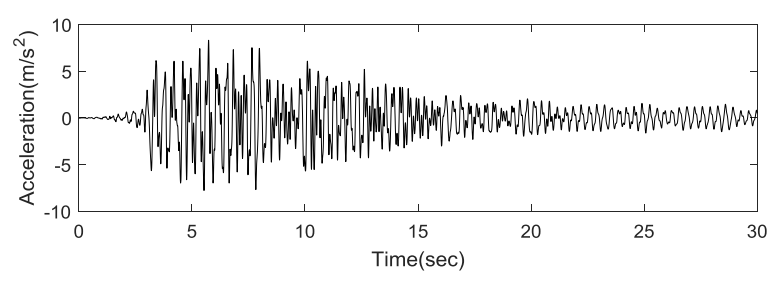


**Fig. 3.** Acceleration response at the top floor.



# Newsletter

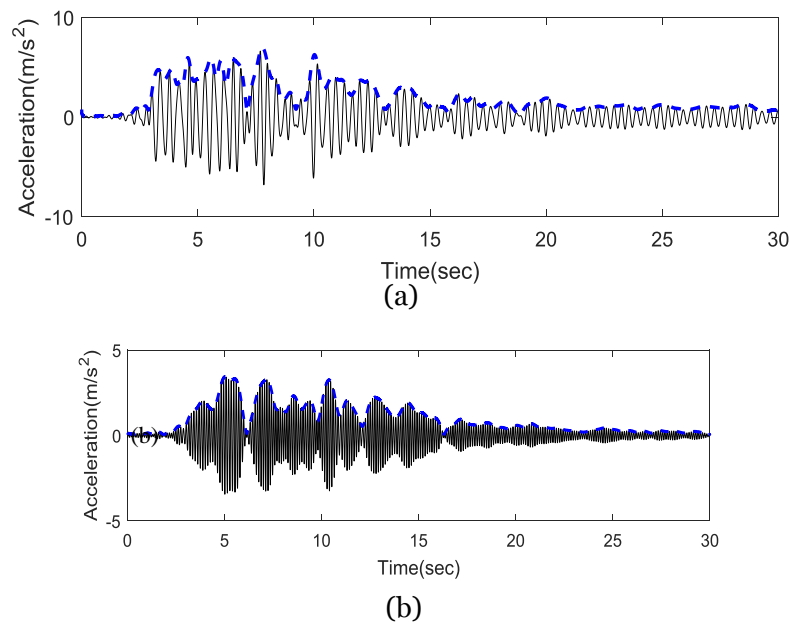


**Fig. 4.** The identified instantaneous amplitudes of the first two mono-components of acceleration response at the top floor: (a) the first component; (b) the second component.

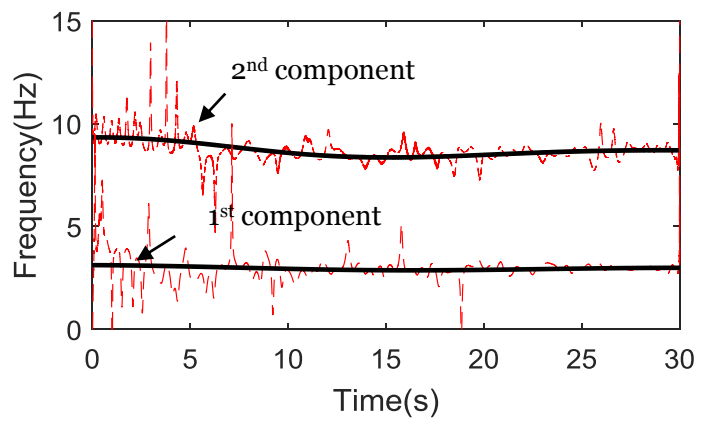


**Fig. 5.** The identified instantaneous frequencies of the first two mono-components.

### Bayesian based nonlinear model updating

In Section 3.1, both the instantaneous frequencies and amplitudes of the first two mono-components are extracted by using AMD method with Hilbert transform, which can be used for nonlinear model updating. Before investigating the performance of nonlinear model updating with these selected data points, the assumption made in Section 2.2 with the difference vector  $\epsilon^m(\theta, t)$  considered as a Gaussian white noise process when the white noises are smeared in the measured data will be



# Newsletter

validated first. The simulated acceleration response on the top floor added with various white noise levels is used for the identification.

Based on the previous studies on nonlinear model updating with Bouc-Wen model (Wang et al. 2015), six parameters  $\alpha, \beta, \gamma, \delta_\eta, \delta_v$  and  $n$  are the nonlinear hysteresis model parameters to be identified in this study. Since the parameters of the Bouc–Wen model are not independent, the similar responses may be generated with different combinations of nonlinear model parameters, which may increase the difficulty in solving the optimization problem. To reliably measure the accuracy of the updating results, two error indices  $R_\omega$  and  $R_{acc}$  are defined as

$$R_\omega = \frac{\|\hat{\omega}(t) - \omega(t)\|_2}{\|\omega(t)\|_2} \times 100\% \quad (9)$$

$$R_{acc} = \frac{\|\hat{A}(t) - A(t)\|_2}{\|A(t)\|_2} \times 100\% \quad (10)$$

in which  $\hat{\omega}(t)$  and  $\omega(t)$  represent the slowly-varying parts of the instantaneous frequencies of the analytical and testing models, respectively;  $\hat{A}(t)$  and  $A(t)$  are the acceleration amplitudes of the analytical and testing models, respectively.  $\|\dots\|_2$  represents the second-norm.

In this study, based on the previous experience of nonlinear model updating (Wang et al. 2015), 5% data points uniformly selected from the amplitudes of decomposed acceleration response are used for nonlinear model updating. The initial model parameters are set

as:  $\theta_{initial} = [1.3\alpha^{true}, 0.5\beta^{true}, 0.5\gamma^{true}, 1.2\delta_\eta^{true}, 0.5\delta_v^{true}, 1.2n^{true}]$ , and the range of those six model parameters

is defined as:  $0.5\theta^{true} \leq \theta \leq 1.5\theta^{true}$ . The error variance of the first component  $\sigma_1^2$  is selected as the error variance of Bayesian method for nonlinear model updating. The initial error variance is set as  $0.2\sigma_1^2$ , and the range of the  $\sigma_1$  is defined as:  $0.01\sigma_1^2 \leq \sigma^2 \leq 100\sigma_1^2$ .

To further study the noise effect, the simulated accelerations with 5%, 10% and 20% white noises are used for the identification analysis, respectively. The updated nonlinear parameters are presented in Table 1, and the errors are shown in Table 2. It can be seen from Tables 1 and 2 that the proposed approach can accurately identify the nonlinear model parameters when measurement noise levels are 5% and 10% with the maximum relative error in the parameter identification less than 10%. For the case with 20% noise, the maximum value of the defined error indices is less than 15% and the maximum relative error in the parameter identification is 30% for the parameter  $\delta_\eta$ . The uncertainty quantification results of these six parameters are listed in Table 3 when different noise levels are

# Newsletter

considered. It can be found that the covariance of the parameter identification results gradually increase with the measurement noise level, which is reasonable and expected. The convergence processes of the six Bouc-Wen model parameters in these three cases are shown in Fig. 6 (a)-(f). A large number of iterations is usually required for the case with a higher noise in the measurement data. A comparison between the acceleration responses with 5% noise effect and the analytical response calculated with the updated parameters are shown in Fig. 7(a). The extracted instantaneous frequencies of the first mono-component are shown in Fig. 7(b). These results also validate that an accurate parameter identification is achieved with the proposed approach.

**Table 1.** Identified parameters of the nonlinear hysteretic model under different noise levels.

Parameters	$\alpha/\alpha^{true}$	$\beta/\beta^{true}$	$\gamma/\gamma^{true}$	$\delta_\eta/\delta_\eta^{true}$	$\delta_v/\delta_v^{true}$	$n/n^{true}$
Exact	1	1	1	1	1	1
5% Noise	0.99	0.96	1.02	1.03	1.01	1.00
10% Noise	1.00	1.04	0.96	1.09	0.98	1.00
20% Noise	0.90	0.99	0.95	1.31	0.89	1.01

**Table 2.** The error indices under different noise levels

	$R_{acc}(\%)$	$R_\omega(\%)$	$\sigma_1/\sigma_1^{real}$
5% Noise	4.51	0.10	1.03
10% Noise	8.32	1.72	0.94
20% Noise	14.9	2.46	1.09

# Newsletter

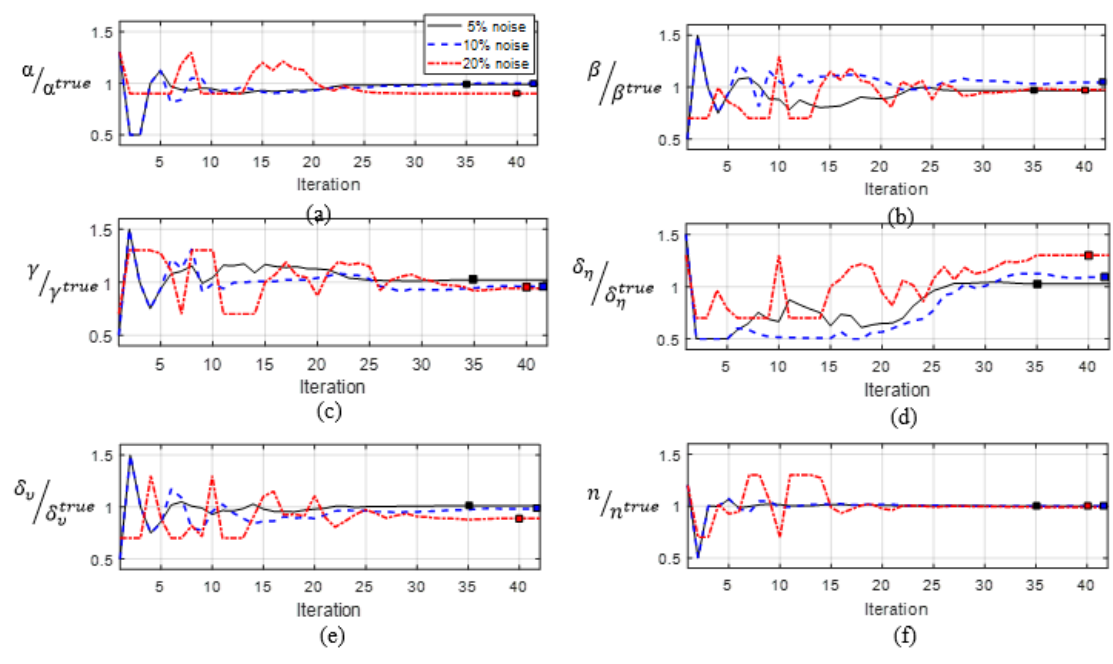
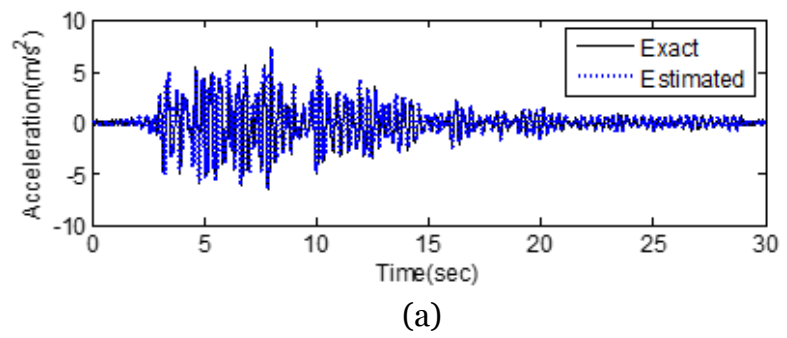


**Fig. 6.** The convergence processes of model parameters under different measurement noise levels.

**Table 3.** Uncertainty quantification of identified nonlinear parameters under different noise levels.

Noise	$cov_{\alpha}(\%)$	$cov_{\beta}(\%)$	$cov_{\gamma}(\%)$	$cov_{\delta_{\eta}}(\%)$	$cov_{\delta_v}(\%)$	$cov_n(\%)$
5%	0.21	0.52	0.49	2.07	0.37	0.05
10%	0.29	0.81	0.59	2.94	0.50	0.05
20%	1.12	3.16	2.96	12.61	2.17	0.22



# Newsletter

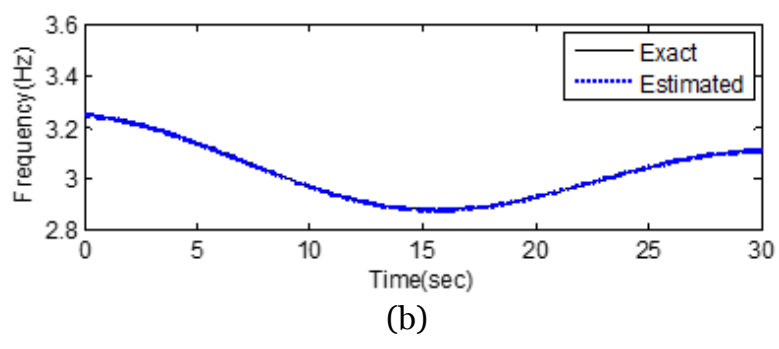


**Fig. 7.** Comparison of the calculated acceleration response and identified instantaneous frequency of the first mono-component from the exact analytical and updated nonlinear models with 5% measurement noise: (a) Acceleration response; (b) Instantaneous frequency.

**Conclusions**

This paper proposes a nonlinear model updating approach based on the instantaneous characteristics of the decomposed structural dynamic responses. The instantaneous frequencies and amplitudes of decomposed acceleration response are extracted by using AMD method. The Bayesian theory is used to quantify the covariance of the updated nonlinear model parameters by using an extended MLE based on the instantaneous amplitudes of decomposed acceleration responses. Numerical studies on a three-story nonlinear shear type building are performed to verify the accuracy and performance of the proposed approach. The results demonstrate that the proposed approach can accurately update the nonlinear model parameters, and is capable of quantifying the uncertain noise effect in the measurements on the nonlinear model updating results.

**ACKNOWLEDGEMENT**

The work described in this paper was supported by Chinese Scholarship Council Postgraduate Scholarship, and Curtin top-up scholarship.

**References**

Beck, J.L., & Katafygiotis, L.S. (1998). Updating Models and their Uncertainties. I: Bayesian Statistical Framework. *ASCE Journal of Engineering and Mechanics*. 12: 44, 455-461.

Behmanesh, I., Moaveni, B., Lombaert, G., & Papadimitriou, C. 2015. Hierarchical Bayesian model updating for structural identification. *Mechanical Systems and Signal Processing*. 64-65: 360-376.

Byrd, R., Gould, N., Nocedal, J., & Waltz, R. (2004). An active-set algorithm for nonlinear programming using linear programming and equality constrained sub-problems. *Mathematical Programming*. 100: 27-48.



# Newsletter

- Feldman, M. (1994). Non-linear system vibration analysis using Hilbert transform—free vibration analysis method. *Mechanical Systems and Signal Processing*. 8:2, 119-127.
- Friswell, M.I., & Mottershead, J.E. (1995). *Finite element model updating in structural dynamics*. The Netherlands: Kluwer Academic Publishers.
- Hemez, F.M., & Doebling, S.W. (2014). Review and assessment of modal updating for nonlinear, transient dynamics, *Mechanical Systems and Signal Processing*. 15:1, 45-74.
- Ikhouane, F., Hurtado, J.E., & Rodellar, J. (2007). Variation of the hysteresis loop with Bouc-Wen model parameters. *Nonlinear Dynamics*. 48:4, 39-41.
- Katafygiotis, L.S., & Beck, J.L. (1998). Updating Models and their Uncertainties. II: Model Identification. *ASCE Journal of Engineering and Mechanics*. 124:4, 463-467.
- Kay, S.M. (1993). *Fundamental of Statistical Signal Processing Volume 1: Estimation Theory*, Prentice Hall, Upper Saddle River, NJ.
- Matlab Optimization Toolbox, User's Guide, R2017a.
- Noel, J.P., & Kerschen, G. (2017). Nonlinear system identification in structural dynamics: 10 more years of progress. *Mechanical Systems and Signal Processing*. 83:2-35.
- Simoen, E., Papadimitriou, C., & Lombaert, G. (2013). On prediction error correlation in Bayesian model updating. *Journal of Sound and Vibration*. 332: 4136-4152.
- Wan, H.P., & Ren, W.X. (2015). Stochastic model updating utilizing Bayesian approach and Gaussian. *Mechanical Systems and Signal Processing*. 70-71: 245-268.
- Wang, Z.C., & Chen, G.D. (2013). Analytical mode decomposition of time series with decaying amplitudes and overlapping instantaneous frequencies. *Smart Materials and Structures*. 22: 095003.
- Wang, Z.C., Xin, Y., & Ren, W.X. (2015). Nonlinear structural model updating based on instantaneous frequencies and amplitudes of the decomposed dynamic responses. *Engineering Structures*. 100: 189-200.
- Xia, Y., Hao, H., Brownjohn, J.M.W., Xia, P.Q. (2002). Damage identification of structures with uncertain frequency and mode shape data. *Earthquake Engineering and Structural Dynamics*. 31:5, 1053-1066.
- Yuen, K.V., & Kuok, S.C. (2011). Bayesian methods for updating dynamic models. *ASME Journal of Applied Mechanics*. 64:1, 010802-1-010802-18.

# Newsletter

## A Technical Note on Remote Sensing for Bridge Monitoring

Mehrisadat Makki Alamdari<sup>1</sup>, Kamyar Kildashti<sup>2</sup>, Linlin Ge<sup>1</sup>, Yincai Zhou<sup>1</sup>

<sup>1</sup>School of Civil and Environmental Engineering, UNSW, Australia.

<sup>2</sup>Western Sydney University, Australia.

### Abstract

In this paper, non-contact sensing is adopted to monitor the health state of a cable-stayed bridge. Displacement influence line (DIL) of the bridge is remotely identified through several field investigations under the live load tests. DIL is simultaneously obtained for a discrete number of target points once the bridge is in its intact condition. Three different remote sensing techniques including, the laser scanning, terrestrial robotic total station and digital levelling are adopted for this purpose which provides a low-cost and easily deployable monitoring system. A damage is emulated on the bridge by locating large stationary mass on the bridge to change the condition of the bridge. A drop of only 1% is observed in the fundamental frequency of the bridge as a result of the induced change. DIL of the damaged bridge is remotely identified and the change in DIL is employed as damage indicator. It is demonstrated that DIL is a robust indicator of change in bridge condition and can be used for detection and localization purpose.

### Bridge monitoring survey

A short-span cable-stayed bridge over the Great Western Highway near Penrith in the state of New South Wales, Australia (33°45'50.49"S, 150°44'31.14"E in WGS84) has been considered. The cable-stayed bridge as illustrated in Figure 1 has a single A-shaped steel tower with a composite steel-concrete deck. The bridge is composed of 16 stay cables with semi-fan arrangement. The bridge span and the tower height are 46 m and 33 m, respectively. This bridge provides a connection between two Western Sydney University campuses over the Great Western highway and carries one traffic lane and one sidewalk. The deck has a thickness of 0.16 m and a width of 6.3 m and is supported by four I-beam steel girders. These girders are internally attached by a set of equally-spaced floor beams as depicted in Figure 1 (c). A dense array of contact-based sensing system, including strain gauge and accelerometer sensors has been deployed on this bridge since July 2016.

# Newsletter



(a) Top view (screen captured from Google Maps).



(b) Side view.



(c) I-shape steel beams and girders beneath the bridge.

**Fig 1.** A cable stayed bridge over the Great Western Highway in NSW Australia.

Four stay cables on each side of the bridge are attached into one end of the 4 beams to support the girders and the bridge deck. The eastern ends of the beams were selected to be monitored for their vertical displacements with various loadings. Ideally, survey targets can be directly attached onto the beam tips. In reality, it is too difficult to attach survey targets on to the end of a beam due to safety issues and risks to drivers on the Great Western Highway. Hence, survey targets are mounted on the

# Newsletter

top of the eastern side rail directly above each beam at points C, D, E and F as illustrated in Figure 2. Points A, B and G are reference targets for the vertical displacement survey of points C, D, E and F.

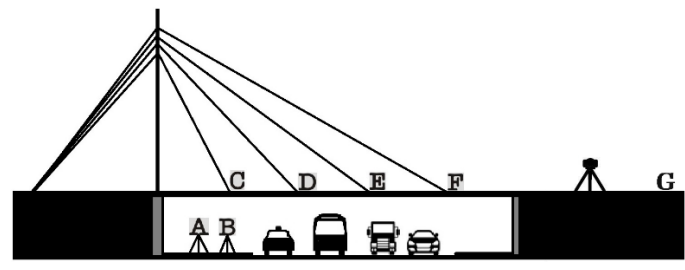


**Fig 2.** Layout of monitoring system.

Three surveying techniques, digital levelling, robotic total station survey and laser scanning, were used to remotely sense vertical displacements of the bridge at the selected 4 points. Levelling staves, circular prisms and laser targets are mounted next to each other at each point with maximum 20 cm horizontal offset to the joint of cable and beam. Once the survey targets are mounted on the bridge rail securely, the targets can be monitored remotely. Detailed instrument and target setups are given in the following sections. A pre-test baseline was surveyed while the bridge has no loadings on it before the test. A post-test baseline survey is done at the end of the monitoring with all loadings are removed. Two tests and 9 cases each were carried out with a time span of 3 hours from 11:30am to 2:30pm on a sunny, light wind and temperature between 20-25 °C.

Two comprehensive static deformation surveys were conducted on the bridge on Saturday 21st of April 2018 with a group of 9 staff and students from UNSW and WSU. Survey 1 was using an eight-ton truck stopping at 9 designated locations on the bridge to survey displacements on the four points. A truck stops at the same 9 locations while the eight-ton truck is parked near point C and close to eastern side rail for Survey 2. Hence, 9 cases for each proposed survey were carried out for the bridge deformation with static loadings on it. Two trucks were adopted in this static bridge deformation survey. Truck 1 is a Test Truck with gross weight of 13.7 ton. Truck 2 is lighter than truck 1 to simulate a damage truck for the survey. In this paper, it is named as Damage Truck with front axle weight of 3.22 tons, rear axle weight of 5.38 tons, gross weight of 8.6 tons and axle distance of 5.3 m.



# Newsletter



Truck 1 – test truck



Truck 2 – damage truck

**Fig 3.** Trucks used for deformation monitoring project.

10 lines were drawn on the bridge, i.e. L1, L2, ..., L10. The distance between every two lines is 5.3 m. The first line is the reference line for all the measurements and it is located on top of the expansion joint at the southern end of the bridge. The distances of L2, L3, ..., L10 from L1 (the reference line) are 0, 5.3 m, 10.6 m, 15.9 m, 21.2 m, 26.5 m, 31.8 m, 37.1 m, 42.4 m and 47.7 m, respectively as indicated in Figure 4 below. Survey targets mounted locations are given in Table 1.



**Fig 4.** Marked lines on the bridge for loading locations.

**Table 1.** Survey targets mounted locations.

Survey Targets	Staff C	Prism C	Prism D	Laser TD	Staff D	Laser TE	Prism E	Staff E	Prism F	Staff F
Distance from reference line (m)	10.21	14.58	21.51	21.81	22.05	29.86	30.13	30.34	38.35	38.51



**Fig 5.** Survey targets on bridge.

# Newsletter

The test truck was used for survey 1 with 9 designed different truck locations on the bridge to align with lines L2, L3, ..., L10. After the pre-test baseline displacement at C, D, E and F was surveyed by the 3 surveying techniques, the test truck was moved to line L2 and parked. Within a few minutes, the targets at point C, D, E and F are surveyed. Then the test truck is moved to the next line sequentially until line L10. Totally 9 tests were conducted on the bridge for survey 1 between 11:30am and 12:45pm. During this survey, the bridge was entirely closed so all the tests are in sequence without any traffic interruption.

Another 9 tests like the ones in Survey 1 were conducted once the damage truck was sitting on the bridge. The location of the front axle and the rear axle from the reference (expansion joint in the south end) is, respectively, 9.87 m and 15.31 m which is approximately between cables 1 and 2 as shown in Figure 6. The damage truck is sitting on the east side of the bridge to provide enough space for the test truck to drive over the bridge on west side. No interruption happened during these tests as the bridge was remained closed for traffic.



**Fig 6.** Location of the damage truck.

Once damage truck was sitting there, the survey was repeated in a similar way to survey 1. It was completed between 12:50pm and 2:30pm.

**Sensing Using Digital Level**

A precise Trimble DiNi22 digital level was used to survey the bridge deformation while different loadings are placed at different locations on the bridge. Digital level is a precise surveying technique to measure height differences among different points. Usually, surveyors use the combination of a digital level and two levelling coded staves to determine height changes from one point to the other. A digital level automatically provides a very precise level line of sight through its telescope to a levelling staff and processes the video information from coded staff to read the height of the staff. The difference between the staff height is the height difference between the two points.

In this levelling survey, five coded levelling staves were securely fixed at points C, D, E, F on the bridge and G on a large concrete base of a road sign. The levelling staff at G is used as a backsight staff



# Newsletter

and a reference as well. The digital level was set between F and G at 20 m from F on the road shoulder. The distances from the levelling instrument to G, F, E, D and C are approximately 10 m, 20 m, 28 m, 36 m and 44 m, respectively. The procedure of the levelling for each displacement survey is sequentially reading staves at G (backsight), C, D, E and F (foresights) two to five rotations. The reference staff G is not necessary if the digital level remain stable on the ground. However, instrument height may be changed due to temperature changes, it's weight over soft soil or accident removal. Hence the reference staff at G is critical to check if any vertical movement of the digital level occurred during the levelling survey. Indeed, the digital level had to be relocated once during the experiment because of blocked line of sight by the simulated damaged truck parked at point C. One may argue about the collimation error due to the distance differences between backsight and the foresights. The collimation errors will be cancelled in the calculated displacements at the four points on the bridge.

Due to the digital level was relocated in the middle of the survey, the height differences from C, D, E and F to G are used to calculate the bridge displacements at the four points. If  $H_{ci}$  and  $H_{gi}$  are readings from staff C and G respectively, the height difference from G to C is  $h_{ci} = H_{ci} - H_{gi}$ . Hence, the mean height difference will be  $hc = \sum_{i=1}^n h_{ci}$ , where n is the number of repeated readings on both staves. The pre-test baseline height differences to G were measured while the bridge has no loads on it. By assuming the displacements of the baseline values are all 0, the absolute displacements of the 4 points for each case will be  $hc - hc_{base}$ . The calculated displacement results for Test 1 and 2 are shown in Figures 7 and 8, respectively.

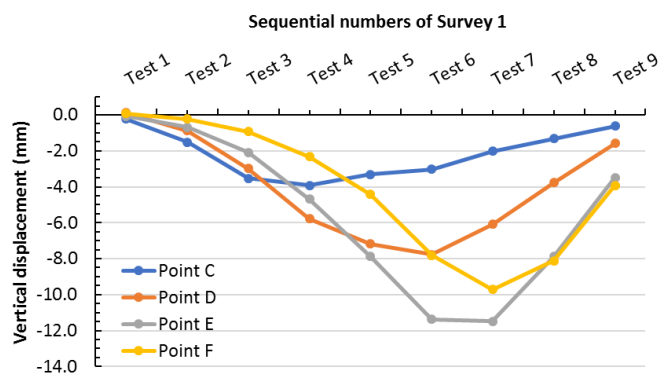


**Fig 7.** Test 1 results: each line represent the displacements and changes at the designed 9 different locations.



# Newsletter

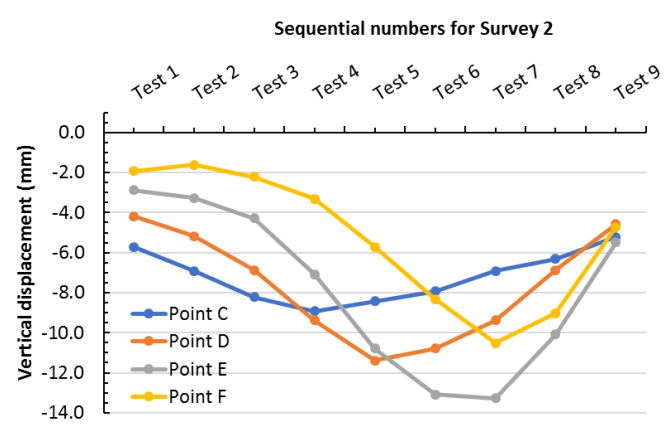


**Fig 8.** Test 2 results: each line represent the displacements and changes at the designed 9 different locations with the damage truck parked near point C.

The post-test baseline survey was carried out between 15 and 20 minutes after the bridge was cleared. The bridge did not recover back to its pre-test state in the 20 minutes. It displaced downward 0.6 mm, 0.5 mm, 0.7 mm and 0.7 mm at point C, D, E and F, respectively.

Specifications for the digital level quote the accuracy of reading error on the staves is  $\pm 0.3$  mm at 40 m distance. The reading error estimation of this survey are  $\pm 0.11$  mm,  $\pm 0.14$  mm,  $\pm 0.21$  mm,  $\pm 0.25$  mm in 1 standard deviation. The computed vertical displacement accuracy is estimated based on error propagation in least square theory. The errors of the vertical displacements for points C, D, E and F are  $\pm 0.12$  mm,  $\pm 0.16$  mm,  $\pm 0.25$  mm,  $\pm 0.29$  mm respectively.

### Sensing Using Total Station

A Leica TCRP 1203+ R400 robotic total station and 5 GPR1 circular prisms were used. One of the GPR1 prism was set up on a tripod under the bridge as reference, at location A. Four (4) prisms were mounted on the bridge rail at points C, D, E and F. The total station was setup at the same side of the highway as prism target A and approximately 15 m away from the bridge. The 5 prisms are surveyed using automatic target recognition (ATR) method with face left observations from A to F and then face right from F to A in sequence. The location coordinates of the 5 points are measured and recorded in the instrument internal memory. The distances from the total station to the targets are less than 50 m. The position accuracy in this survey is  $\pm 1$  mm according to the instrument's specification in the Leica TPS1200+ User Manual. The vertical location precision, i.e. relative accuracy of multiple measurements to the same prism was also quantified in the filed with 24



# Newsletter

measurements to each of the prisms. The standard deviation of vertical heights are  $\pm 0.49$  mm,  $\pm 0.68$  mm,  $\pm 0.51$  mm,  $\pm 0.58$  mm and  $\pm 0.69$  mm for points A, C, D, E and F. Hence, the precisions of the calculated displacements of points C, D, E and F are  $\pm 0.83$  mm,  $\pm 0.71$  mm,  $\pm 0.76$  mm and  $\pm 0.85$  mm, respectively. The calculated displacement results from the total station measurements are given in Figures 9 and 10 for survey 1 and survey 2, respectively.

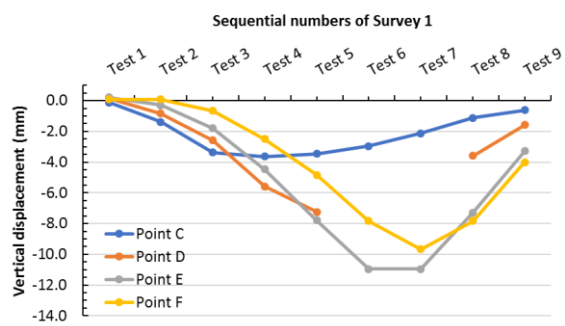


**Fig 9.** Test 1 results: each line represent the displacements and changes at the designed 9 different locations.

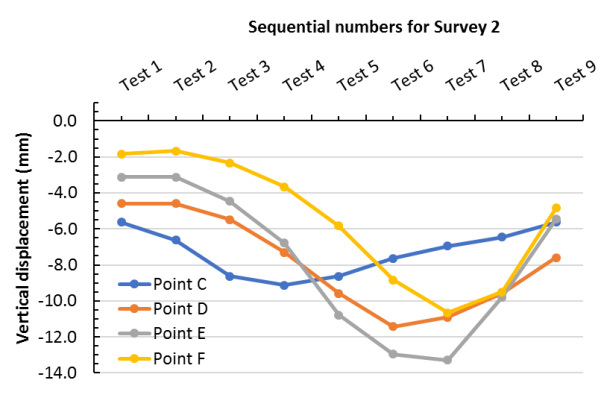


**Fig 10.** Test 2 results: each line represent the displacements and changes at the designed 9 different locations with the damage truck parked near point C.

## Sensing Using Laser Scanner

A Leica ScanStation C10 terrestrial laser scanner was used with 3 algorithmic fit to planar HDS targets. A 3"x3" square planar target was set up on a tripod under the bridge as a reference. Two 6" circular planar targets, were mounted on the bridge at locations D and E, respectively. Leica's HDS targets allow intelligent, automatic identification and extraction by Cyclone software with its carefully designed differences in reflectivity between the target centre and the main target surface, plus tight manufacturing tolerances. The precision of vertical location from a single target scan on the planar



# Newsletter

HDS targets was evaluated from multiple scans to the reference target B. The standard deviation of its precision is  $\pm 0.28$  mm even though the target acquisition accuracy is stated as  $\pm 2$  mm standard deviation in Leica’s product specification. The displacements of D and E are calculated by comparing to the baseline measurements. Hence the calculated displacement precision is  $\pm 0.40$  mm according to error propagation in least square theory. The surveyed displacement results are given in Figures 11 and 12.

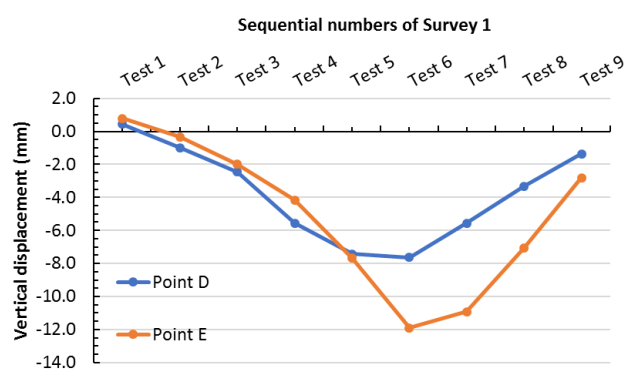


**Fig 11.** Test 1 results: each line represent the displacements and changes at the designed 9 different locations.

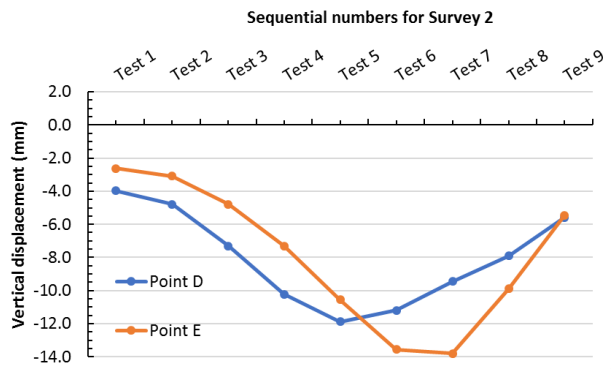


**Fig 12.** Test 2 results: each line represent the displacements and changes at the designed 9 different locations with the damage truck parked near point C.

## Acknowledgement

The authors wish to thank the Road and Maritime Services (RMS) in New South Wales, Western Sydney University and Datat61|CSIRO (former National ICT Australia (NICTA)) for provision of the support and testing facilities for this research work.



# Newsletter

## Conference News

- **11th ANSHM Annual Workshop, Griffith University, 2-3 December 2019, Gold Coast.**  
<https://www.griffith.edu.au/cities-research-institute/news-and-events/seminars-and-events/11th-anshm-annual-workshop>.
- **10th International Conference on Bridge Maintenance, Safety, and Management, MS06: Bridge Loading – Measurement and Modelling, June 28- July 2 2020, Japan.** <http://www.iabmas2020.org/>
- **9th International Conference on Structural Health Monitoring of Intelligent Infrastructure, 4-7 August 2019, St. Louis, Missouri, USA.** <https://shmii-9.mst.edu/>.
- **16th East Asia-Pacific Conference on Structural Engineering & Construction (EASEC-16), 3rd-6th Dec 2019, Brisbane, Australia.** (<https://easec16.com.au/>)

## Social Media

Follow us at the next social media and webpages

- ANSHM Facebook webpage: [www.facebook.com/ANSHMAU](http://www.facebook.com/ANSHMAU)
- ANSHM Facebook group: [www.facebook.com/groups/ANSHM](http://www.facebook.com/groups/ANSHM)
- ANSHM LinkedIn group:

[www.linkedin.com/groups/ANSHM-Australian-Network-Structural-Health-4965305](http://www.linkedin.com/groups/ANSHM-Australian-Network-Structural-Health-4965305)

If you have any comments and suggestions, please contact

Newsletter Editor: Mehrisadat Makki Alamdari, University of New South Wales.

Email: [m.makkialamdari@unsw.edu.au](mailto:m.makkialamdari@unsw.edu.au)

Co-Editors:

Jun Li, Curtin University

Richard Yang, Western Sydney University